Comparing the effect of geometry and stiffness on the effective load paths in non-symmetric laminates

Sergio A. Minera Rebulla*, Mayank Patni†, Paul M. Weaver‡,
Alberto Pirrera§, and Matthew P. O'Donnell¶
Bristol Composites Institute (ACCIS), University of Bristol, Queen's Building, Bristol UK, BS8 1TR

In aerospace composite material design, it is common to encounter load bearing components that vary in thickness across their length. In plate design, ply drops, tow-steering, and the addition of stiffeners, all act to change both the section geometry and the effective stiffness of the part. Often, due to aerodynamic design constraints, the geometric profile must transition non-symmetrically, i.e. thickness is built up from a reference surface, meaning the mid-surface of the plate does not remain on a constant plane. These localised changes in geometry, and associated change of position of the mid-surface, lead to inherently three-dimensional states of stress. As a consequence, and especially for composite structures, there is the potential for significant through-thickness stresses and/or stress concentrations, leading to failure—for example debonding or delamination. By investigating the effects of geometric and effective stiffness changes, we are able to gain physical insight into structural behaviour in the regions of geometric transition. This is achieved through a parametric study, whereby we compare the behaviour as predicted by Classical Laminate Theory—a commonly utilised two-dimensional approach—with a finite element analysis based on the Unified Formulation by Carrera and co-workers. Based on these investigations, we are able to illustrate how rates of profile change and/or stiffness variation are linked to variance in the predicted location of the neutral plane of the two approaches which acts as a proxy measure for predicting through-thickness behaviour. Finally, we discuss the potential opportunity to utilise laminates that possess non-standard layups to tailor the load path through geometric transitions, thus offering a potential route for elastic tailoring that minimises undesirable through-thickness stresses.

I. Introduction

LAMINATED composite materials are utilised within aerospace design for their high strength to weight ratio, geometric tailor-ability, and their anisotropic properties that may be aligned with critical load paths. These promising characteristics are responsible for their significantly increased utilisation; for example, the Boeing 787 and Airbus A350 have composite materials exceeding 50% of their structural weight [1]. Despite these desirable characteristics, composites are comparatively sensitive to loads in the through-thickness direction—a characteristic that often becomes a driving factor in design, e.g. stringer terminations [2–4]. Due to this sensitivity to through-thickness stresses, best practice design seeks to minimise the occurrence of sharp geometric changes and to control the locations and pairing of ply drops. In practice, these rules of design cannot always be met; discrete changes in geometric profile and stiffness are often unavoidable in order to meet non-structural requirements e.g. to preserve aerodynamic shape. These changes introduce load paths that have an inherent through-thickness component and should be accounted for in structural analysis, which, in turn, leads to increased analysis time and computational cost.

It is, therefore, essential to the design process that through-thickness effects can be captured using efficient analysis tools. For these reasons, designers are often drawn towards two-dimensional modelling approaches due to their reduced complexity and computational efficiency, when compared to full 3D solid element finite element analysis (FEA). However, this is not without cost. Two-dimensional approaches often condense behaviour to a representative reference plane and in so doing can remove certain geometric and stiffness features, e.g. double lap joints [5]. To mitigate this deficiency, basic two-dimensional approaches are often modified to capture three dimensional geometric effects. One

*Marie Sklodowska-Curie Research Fellow
†Marie Sklodowska-Curie Research Fellow
‡Professor in Lightweight Structures
§Senior Lecturer in Composite Structures - EPSRC Research Fellow
¶Lecturer in Composite Structures Matt.ODonnell@bristol.ac.uk

such example was done by Cosentino and Weaver [6] who developed a non-linear smeared stiffness CLT (Classic Laminate Theory) analysis for stringer terminations with an eccentricity function introduced to account for the large changes in geometry. The same authors then developed this approach further to aid in the preliminary sizing of stringer terminations [7]. This approach assumed *a priori* knowledge of the eccentric load path in the form of a truncated series approximation to smooth geometric and stiffness discontinuities. Herein, we seek to gain further insight into the shape of load paths within structures by considering how rates of change of geometry and stiffness affect its form and smoothness.

As an alternative to computationally expensive 3D FEA, there is significant interest in the use of the Unified Formulation (UF) approach by Carrera and co-workers [8, 9]. Recently, a cross-section finite element based on the Serendipity Lagrange Expansion (SLE) function, developed within the UF framwework, was shown to offer computational benefit over 3D FEM [10]. Moreover, the UF-SLE model provides accurate through-thickness measurements in laminated composites and stiffened structures [11, 12]. This improvement in performance is not without cost and the approach limits the types of structural geometries that can easily be considered, however, it is sufficient for many common aerospace components. In this paper, we seek to explore the limits of modified CLT approaches, in their ability to account for geometric and stiffness variations. In particular, we investigate the effects of eccentricity in the load path for geometrically non-symmetric structures and assess the effects of any associated through-thickness stresses. With this information, we are able to consider bounds that may limit the applicability of commonly used CLT-based analyses for the preliminary design of asymmetrical ply-dropping schemes, variable angle tow laminates with associate thickness variation, and stiffened plate structures.

The current investigation seeks to assess where assumptions of two-dimensional behaviour, in typical aerospace components, break down. In general, geometric variations and stiffness variations are coupled—as you change the thickness of a component its stiffness varies in tandem. To gain insight into this effect and into the ensuing formation of three-dimensional stress fields, we seek to isolate the consequences of geometric and stiffness changes by considering simplified tapers and stiffness variations, whilst still being sufficient to retain crucial features and to provide the most understanding. To simplify the analysis further, we focus on the behaviour in the principle direction of a tapered section, but the results can be readily extended to include more general two-dimensional variations. To aid in the approximations, we consider cross-ply laminates, thereby avoiding bend-twisting and extension-shear couplings. By comparing the strains predicted by modified CLT and the UF-SLE model, we can comment on the length scale over which a change in geometry and/or stiffness can be permitted such that the response remains nominally planar—thereby avoiding unwanted through-thickness loads.

We know from the principle of Saint-Venant that, as you move further from a boundary or discontinuity, its effect on structural behaviour decreases. The distance at which boundary effects can be negated are determined by a variety of factors [13]. When a critical point in the structure corresponds to a localised change in properties, such as a stringer run-out, a ply drop, or an angle change, it is important to understand the effect this has on the strength of the system. As such, it is essential to establish the extent of variation between two-dimensional and three dimensional results. In particular, establishing how behaviour is affected by rates of change of stiffness and geometric properties.

The paper proceeds as follows. An outline of CLT and how it may be utilised to identify the load path through a component with changes in geometric profile is presented. This is followed by a brief introduction to the three-dimensional analysis based on the UF-SLE model as developed by Minera et al. [10]. The paper then considers the neutral plane position in a range of tapered sections with a range of stiffness configurations. We note that the neutral plane's eccentricity through the tapered section may be utilised as a representative predictor for through-thickness loading. The various tapered sections considered are indicative of ply-drops, stringer terminations, and tow-sheared thickness variations. We comment on the accuracy of CLT predictions, compared with UF-SLE, for various stiffness and geometric parameters as a function of their relative rates of change.

II. Classical Laminate Analysis Approach

As is convention, we assume that layers of a laminated composite plate are perfectly bonded to each other, and that the stiffness properties may be condensed to the mid-plane. The mid-plane resultants per unit length, $\mathbf{N}$ and $\mathbf{M}$, are related to the curvatures, $\boldsymbol{\kappa}$, and mid-plane strains, $\boldsymbol{\varepsilon}$, via the $\mathbf{A}$, $\mathbf{B}$, and $\mathbf{D}$ symmetric stiffness matrices, taking their usual definition from CLT [13]:

$$\begin{bmatrix}\mathbf{N}\\ \mathbf{M}\end{bmatrix} = \begin{bmatrix}\mathbf{A} & \mathbf{B}\\ \mathbf{B} & \mathbf{D}\end{bmatrix}\begin{bmatrix}\boldsymbol{\varepsilon}\\ \boldsymbol{\kappa}\end{bmatrix}, \qquad \begin{bmatrix}\boldsymbol{\varepsilon}\\ \mathbf{M}\end{bmatrix} = \begin{bmatrix}\mathbf{a} & \mathbf{b}\\ -\mathbf{b}^{\top} & \mathbf{d}\end{bmatrix}\begin{bmatrix}\mathbf{N}\\ \boldsymbol{\kappa}\end{bmatrix}, \qquad \begin{bmatrix}\boldsymbol{\varepsilon}\\ \boldsymbol{\kappa}\end{bmatrix} = \begin{bmatrix}\mathbf{a}' & \mathbf{b}\mathbf{d}^{-1}\\ \mathbf{d}^{-1}\mathbf{b}^{\top} & \mathbf{d}^{-1}\end{bmatrix}\begin{bmatrix}\mathbf{N}\\ \mathbf{M}\end{bmatrix}, \tag{1}$$

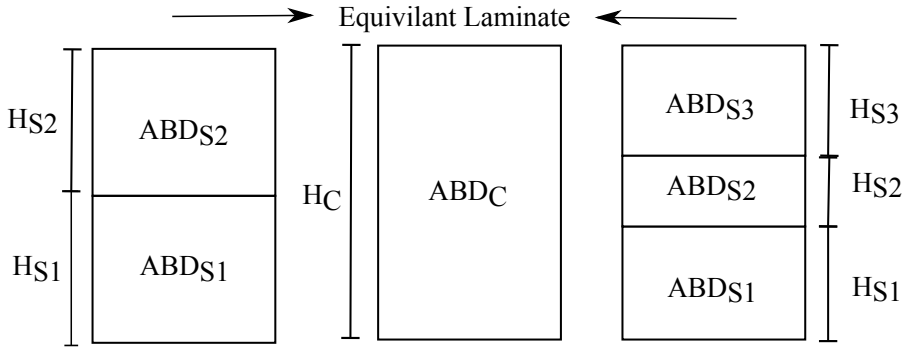

Fig. 1 Combining sub-laminates to obtain the combined properties - for laminates with two or three sub-laminates.

with,

$$\mathbf{a} = \mathbf{A}^{-1}, \qquad \mathbf{b} = -\mathbf{A}^{-1}\mathbf{B}, \qquad \mathbf{d} = \mathbf{D} - \mathbf{B}\mathbf{A}^{-1}\mathbf{B}, \qquad \mathbf{a}' = \left(\mathbf{A} - \mathbf{B}\mathbf{D}^{-1}\mathbf{B}\right)^{-1}. \tag{2}$$

In order to combine two sub-laminates together and obtain the equivalent stiffness properties, $\mathbf{ABD}_{C2}$, see figure 1, we may utilise the following identities [14],

$$\begin{aligned}
\mathbf{A}_C &= \mathbf{A}_{S1} + \mathbf{A}_{S2}, \\
\mathbf{B}_C &= \mathbf{B}_{S1} + \mathbf{B}_{S2} - \frac{H_{S2}}{2}\mathbf{A}_{S1} + \frac{H_{S1}}{2}\mathbf{A}_{S2}, \\
\mathbf{D}_C &= \mathbf{D}_{S1} + \mathbf{D}_{S2} - H_{S2}\mathbf{B}_{S1} + H_{S1}\mathbf{B}_{S2} + \frac{H_{S2}^2}{4}\mathbf{A}_{S1} + \frac{H_{S1}^2}{4}\mathbf{A}_{S2},
\end{aligned} \tag{3}$$

where H_{S1}, $\mathbf{ABD}_{S1}$ and H_{S2}, $\mathbf{ABD}_{S2}$ are, respectively, the thickness and stiffness properties of the first and second sub-laminates.

It is evident that combining two symmetric sub-laminates does not guarantee a globally symmetric total laminate. If we consider the addition of a single ply as sub-laminate two, i.e. addition of a new outer ply, then the total layup becomes non-symmetric*, and depending on the relative stiffness of the additional ply to the original layup can introduce significant **B** coupling effects. We can employ the sub-laminate formula consecutively to obtain an equivalent formula for a three sub-laminate laminate. Of particular interest is the formula for the **B** coupling terms,

$$\mathbf{B}_C = \mathbf{B}_{S1} + \mathbf{B}_{S2} + \mathbf{B}_{S3} - \frac{H_{S2} + H_{S3}}{2}\mathbf{A}_{S1} + \frac{H_{S1} - H_{S3}}{2}\mathbf{A}_{S2} + \frac{H_{S2} + H_{S3}}{2}\mathbf{A}_{S3}, \tag{4}$$

from which we can interpret the effect of including/dropping an additional ply at any position in the stack. We can observe that unless the ply is included symmetrically about the mid-plane then, in general, **B** coupling is introduced into the system. It is for this reason that designers recommend ply-drops typically occur in pairs, located at identical distances from the mid-plane.

The existence of **B** terms in the stiffness matrix is important as it couples in-plane stretching with out-of-plane bending. It is for this reason that non-symmetric laminates are typically discouraged as the deformation mode becomes more complex. From a physical point of view, stiffness non-symmetry results in the geometric mid-plane and the neutral plane for bending no longer being coincident. In general, there are three neutral planes located z_x, z_y and z_{xy}, from the mid plane which can be determined for a pure bending load as [15],

$$\mathbf{0} = (\mathbf{b} + \mathbf{z}_n)\,\mathbf{d}^{-1}\mathbf{M}, \qquad \text{with} \qquad \mathbf{z}_n = \text{diag}\left(z_x, z_y, z_{xy}\right). \tag{5}$$

From Equation (5), we can observe that the exact position of the neutral plane is affected by the relative intensity of each component of applied moment resultants. Furthermore, we note that in general, $z_x \neq z_y \neq z_{xy}$, meaning that the

*unless sub-laminate one is the corresponding uni-directional laminate

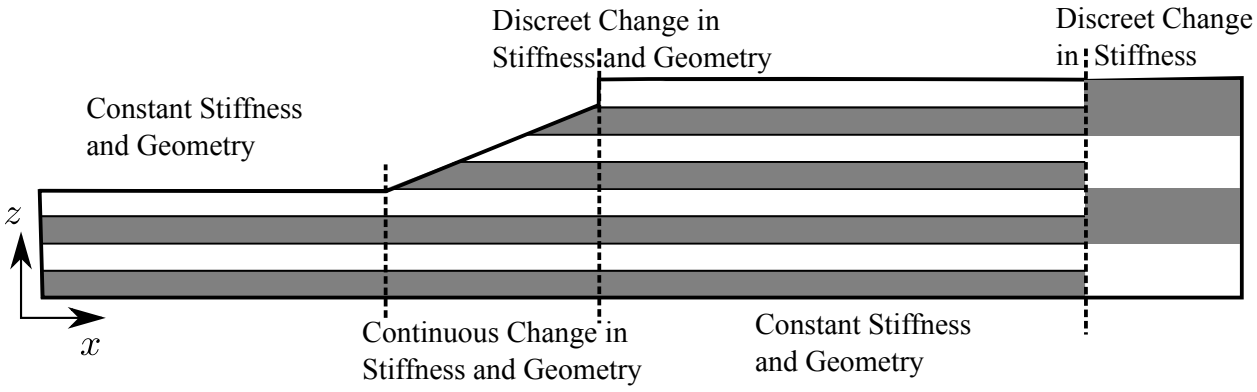

Fig. 2 General prismatic cross section showing regions with both discrete and continuous variations in thickness and stiffness.

effective load paths for each component of loading are not themselves co-located. As an alternative approach, from inspection of the partially inverted form of CLT, equation (1), we observe that moment resultants are related to in-plane stress resultants through $-\mathbf{b}^\top$. Thus, we may interpret this matrix as defining effective lever-arms, or eccentricities, and as a measure of the distance from the mid-plane to the effective loading path. The matrix $-\mathbf{b}^\top$ has, in general, six unique components. However, it is possible to consider each lever arm on a component-wise basis, e.g. the contribution to M_x associated with N_x has a lever-arm determined by $-b_{11}$, etc. By tracking this effective lever-arm measurement, we can assess how the load path varies with changes in geometry and stiffness. This stiffness-only approach has the advantage that it does not depend on the relative intensity of the applied loads, and for the case of cross ply laminates under uniaxial bending, $-\mathbf{b}_{11} = z_x$, i.e. $\mathbf{M} = [M_x, 0, 0]^\top$. Clearly, where there are discrete changes in stiffness and/or geometry, then both approaches to predicting load paths may not provide a continuous load path. This is an inherent limitation of CLT.

We may interpret the neutral plane position as defining the eccentricity of the load-path of in-plane stress resultants through the structure that does not induce moments. Using this approach, we may provide a prediction for through-thickness stresses by assuming that an associated vertical component of loading is induced due to the slope of the eccentricity function and associated load path. Let us consider the behaviour in the x-direction for tapered cross section in figure 2. We note that the load path's position will be defined as a combination of changes in the position of the midsurface, together with any non-symmetric geometric changes, cf. the taper and the effect of non-symmetric stiffness variations due to the introduction of new sub-laminates. Considering figure 3, for shallow tapers the following approximation for the through-thickness resultant due to the in-plane resultant can be made,

$$\begin{aligned} N_v &= N_x \frac{\partial e}{\partial x} \\ e(x) &= \underbrace{\tfrac{1}{2}H(x)}_{\text{geometry}} + \underbrace{z_x(x)}_{\text{stiffness}} . \end{aligned} \tag{6}$$

This equation illustrates how the change in position of the neutral plane can be considered as representative of through-thickness stresses. The effect of geometry on the eccentricity function can be directly obtained by considering the geometric thickness function $H(x)$ and is thus easy to interpret. We note that in order to avoid the effects of a discontinuity caused by the geometric profile the shape need be C^1 smooth. It is for this reason we consider both a linear and cubic shaped taper. The stiffness component requires greater consideration. If we consider the stiffness properties of a combined laminate, equation (3) can be used to calculate the stiffness properties at a ply drop/thickness build up. We note that even for a simple change of total laminate properties, such as that observed in a linear taper, the combined stiffness properties do not vary linearly. In order to calculate the neutral plane's position we must invert the stiffness matrices, meaning that all components of the stiffness matrices affect the position of the load path, in each direction, therefore complicating the relationship further. Examples of this non-linear change in stiffness can be found in the results section IV, which follows the introduction to the Serendipity Lagrange element-based Unified Formulation presented in the following section.

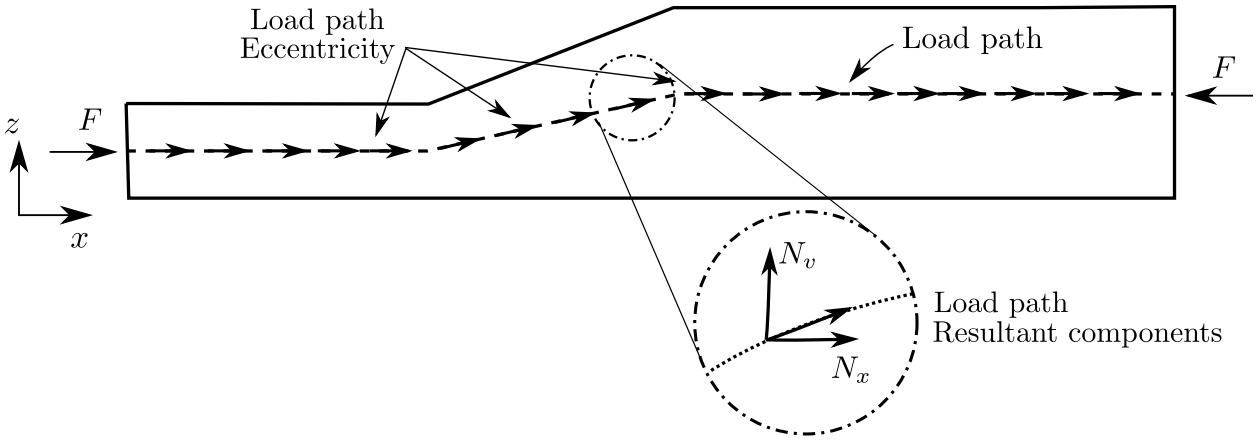

Fig. 3 Load path through a prismatic tapered section indicating how load path eccentricity results in a through-thickness component.

III. Three-Dimensional Analysis framework

When trying to capture through-thickness behaviour of composites it is common practice to utilise 3D FEA. However the increased computational cost when using solid 3D elements is widely recognised. In order to avoid such costly computations, we instead employ the Unified Formulation (UF) framework [9], which relies on a displacement-based formulation of the finite element method. The advantage of a finite element discretization is that arbitrary geometries and boundary conditions can readily be modeled. The three-dimensional displacement field is given as

$$\boldsymbol{u}(x, y, z) = \{u \quad v \quad w\}^{\top}. \tag{7}$$

In the current setting, the longitudinal axis of the structure is discretized with four-noded, Lagrange 1D finite elements, so that the displacement field can be approximated element-wise by means of local shape functions $N_i(x)$, and generalized nodal displacements, $\boldsymbol{u}_i(y, z)$, such that

$$\boldsymbol{u}(x, y, z) = \sum_{i=1}^{4} N_i(x)\boldsymbol{u}_i(y, z). \tag{8}$$

The transverse, or cross-sectional, deformations are approximated using hierarchical Serendipity Lagrange Expansion (SLE) functions $F_\tau(y, z)$. Adopting this expansion model, cross-sections are discretized using four-noded Lagrange sub-domains and the displacement field within each sub-domain can be enriched by increasing the order of the local Serendipity Lagrange expansion. The cross-sectional displacement field at the i^{th} beam node is expressed as

$$\boldsymbol{u}_i(y, z) = \sum_{\tau=1}^{m} F_\tau(y, z)\boldsymbol{u}_{i\tau}, \tag{9}$$

where m is the number of terms depending on the order of expansion and $\boldsymbol{u}_{i\tau}$ are generalized displacement vectors. By introducing the cross-sectional approximation of Eq. (9) into the FE discretization along the beam axis of Eq. (8), the displacement field reads

$$\boldsymbol{u}(x, y, z) = \sum_{i=1}^{4}\sum_{\tau=1}^{m} N_i(x)F_\tau(y, z)\boldsymbol{u}_{i\tau}. \tag{10}$$

A detailed description of this model is not repeated here for brevity and can be found in Minera et al. [10]. The mesh is split into three regions along the beam direction with 10 B4 elements (4-noded Lagrange) in each region. The elements's nodes are distributed in a Chebyshev grid ensuring there is always a node present at any position of discontinuity in stiffness and/or geometry. This approach captures any sharp change in material properties and provides a good distribution of elements near the boundaries and discontinuities. A third order expansion was utilised in the cross-section with one sub-domain per layer. The satisfactory convergence of the solution was ensured by comparison with results obtained with increased mesh refinements and further comparison with 3D Ansys FEA. The UF-SLE based analysis

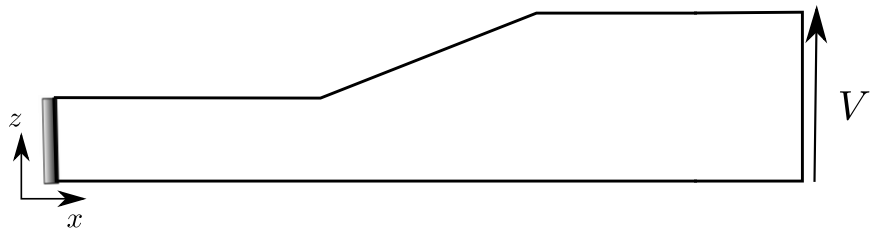

Fig. 4 Loading state utilised to obtain neutral plane's position using the UF-SLE model.

Table 1 Representative Material Properties

ν_{12}	0.288
E_{11}	163.3 GPa
E_{22}	10.79 GPa
G_{12}	5 GPa
H_{ply}	0.131 mm

provides an efficient way of recovering full field behaviour and is applicable to typical geometries observed in structural components. By utilising such an approach for the simple beam-like geometries considered herein we can demonstrate its potential for use in more complex geometric and stiffness tailoring problems that can be investigated in future works.

In order to make a comparison between CLT and UF-SLE based analyses, we are required to obtain a full 3D description of the stiffness properties. Following the approach of Kumar and Shapiro [16], 3D stiffness matrices may be recovered from a given laminate through the use of an equivalent three layer model. Their approach has shown good correlation with numerical tests and is applicable for predicting response characteristics investigated in this paper.

To simplify the comparison we again focus on behaviour in the x-direction only, figure 4. Our structure possesses symmetry boundary conditions replicating the effect of an infinitely wide plate allowing us to determine the behaviour in the x-direction independently of boundary conditions in the y-direction. In order to determine the location of the neutral plane the structure is clamped at $x = 0$ and subject to a unit shear load at the free end, inducing a bending moment along the beam direction. The strain field is then sampled at regular intervals along the beam direction. Figure 5, illustrates a typical strain field. The position of zero strain $\varepsilon_x(z)$ through the thickness at each sample position is then used to determine the effective neutral plane. A similar approach was utilised by Patni et al. [17] to determine the position of the neutral plane for T-sections.

Using the neutral plane eccentricity function obtained from the bending analysis, we are able to compare the predictions of the UF-SLE model with those of CLT.

IV. Comparison of neutral plane

In the following section, we investigate the effective position of the neutral plane in the x-direction for constant thickness geometries, linear taper, and cubic tapers; see figure 6. Details of the stiffness properties and specific parameterisation are described in each of the subsection. We utilise material properties listed in table 1, which are representative of typical carbon-epoxy aerospace composites. When presenting our results, we make the following normalisations to aid comparison of the various taper rates,

$$\tilde{x} = \frac{x - L_1}{cL_1} \qquad \tilde{y} = \frac{y}{H_2} \qquad \tilde{\varepsilon} = \frac{\varepsilon}{\max|\varepsilon|} \tag{11}$$

where c and L_1 and H_2 are defined in figure 6. This normalisation ensures the taper occurs in the non-dimensional range $[0, 1]$ for all slope geometries, and that the height of the full structure varies between $[0, 1]$ with the neutral planes and mid-plane position scaled accordingly. We select L_1 and L_2 to be sufficiently large compared to H_1 and H_2 that behaviour is nominally planar at the edges of the domain allowing us to focus our observations in the regions of geometric and stiffness variation.

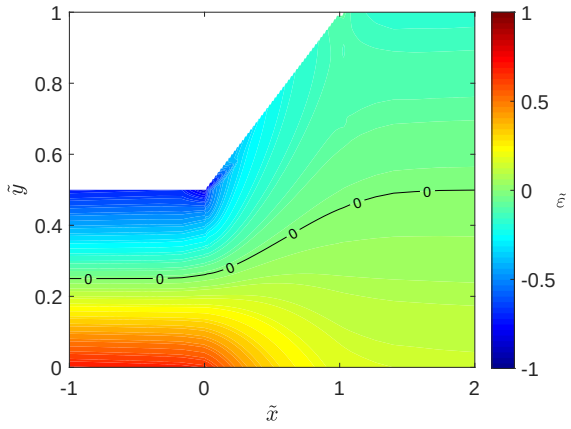

(a) Total layup $[0]_8$ with taper $c = 0.1$

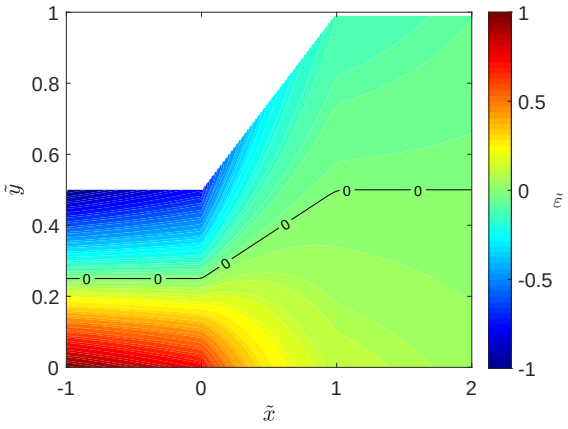

(b) Total layup $[0]_8$ with taper $c = 1$

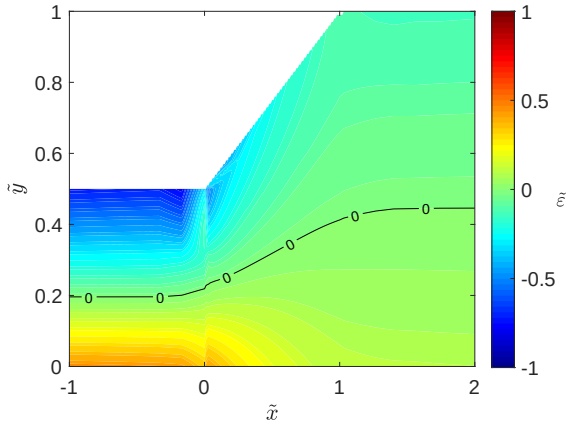

(c) Total layup $[0, 90]_4$ with taper $c = 0.1$

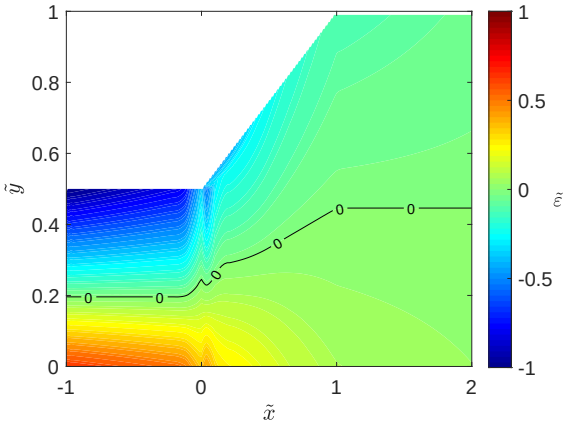

(d) Total layup $[0, 90]_4$ with taper $c = 1$

Fig. 5 Examples of the normalised strain fields $\tilde{\varepsilon}$, for bending load case used to identify span-wise neutral plane. Results obtained by employing the UF-SLE model.

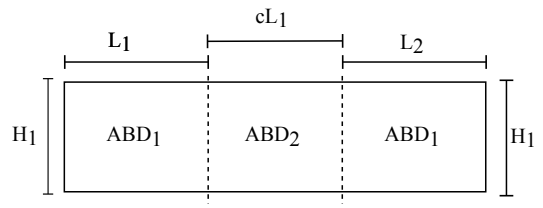

(a) Constant geometry with discrete stiffness variation in middle region.

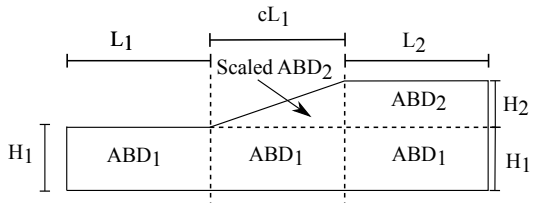

(b) Linear taper with C^0 geometric continuity and scaled stiffness properties through taper.

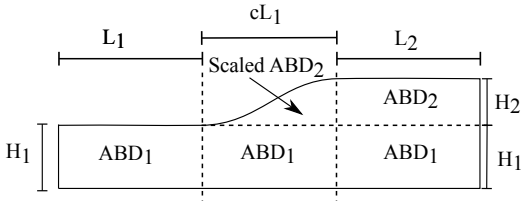

(c) Cubic taper with C^1 geometric continuity and scaled stiffness properties through taper.

Fig. 6 Taper Geometries Considered.

A. No Geometric Variation

The first case study considers a constant thickness geometry, but investigates the effect of a discrete change in layup and therefore stiffness. For a non-symmetric layup, figure 6a, the effective neutral planes and location of the load path changes position relocating in a spanwise direction. As previously discussed, we restrict the analysis to cross-ply laminates to ensure that we can most effectively capture behaviour in one direction. In order to maximise the effect of non-symmetry discontinuities we consider a [0,90] laminate configuration. Figure 7 shows the effective load path as calculated by CLT and UF-SLE with the mid-plane provided for reference. We observe that, since the 0° ply is significantly stiffer that the 90°, the neutral plane changes accordingly. CLT predicts a jump in location of the neutral plane's position. However, the UF-SLE results illustrate the length scale over which the transition actually occurs with an associated smoothing of the load path. Figure 8 illustrates how the UF-SLE normalised strain field, $\tilde{\varepsilon}$ displays a non-linear variation through the thickness in regions close to the boundaries of the material discontinuity, $\tilde{x} = 0$ and $\tilde{x} = 1$. It is this region of non-linearity in the strain field that accounts for the smooth change in position of the neutral plane. We note, that for a modified CLT analysis that included a purely geometric eccentricity function this change in position of the neutral axis would not be captured accurately. Furthermore, by considering figure 7, we observe that for regions with a relatively short taper region, $c = 0.1$, the stiffness modified CLT cannot accurately predict the true neutral plane for significant portions of the domain. Having established the significance of stiffness in modifying the neutral plane we now compare the effects of geometric variation when coupled with stiffness changes.

B. Linear Taper

In this example, the taper varies linearly with a coefficient c as a proportion of the length L_1 that dictates the gradient of the slope. The layup in the thickest region dictates the layup for the whole of the prismatic structure. The effective layup at any given point along the section is determined by the relative height; i.e., if the height is equal to five plies, the layup at that point consists of the first five plies of the total layup. Where the height does not correspond to a complete ply, e.g. 5.5, then a corresponding reduced ply thickness is imposed on the final part, giving the first five plies plus a final half of the sixth.

The examples considered allow us to investigate the effects of non-symmetric stiffness distributions within the taper. We note that although the thin and thick regions are symmetric the taper's stiffness distribution is, in general, non-symmetric.

We observe in figure 9a, that the trend lines tend towards the geometric midplane. We note that for the sharper tapers the neutral plane position is raised before the onset of the taper and reduced upon its completeness. In essence,

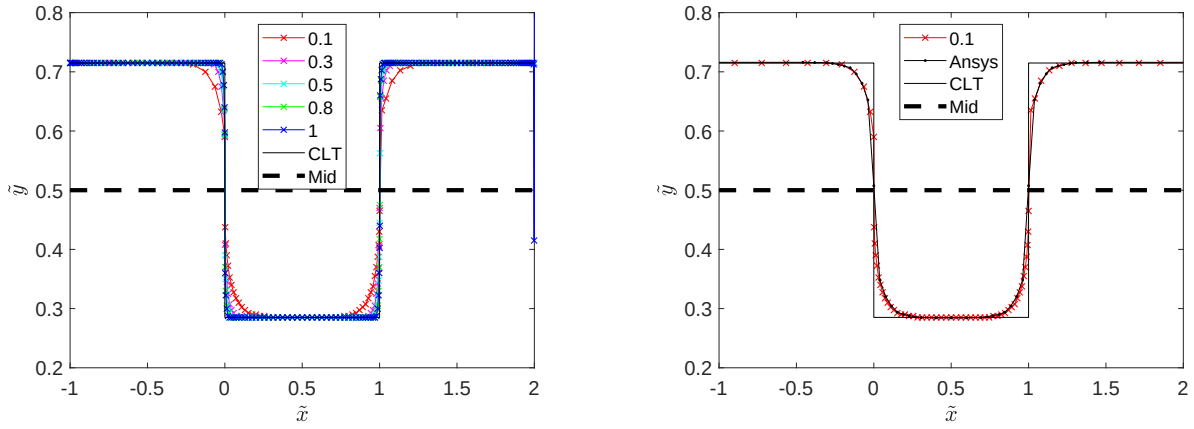

(a) UF-SLE predictions of neutral plane. **(b) Comparison of UF-SLE with Ansys for $c = 0.1$.**

Fig. 7 Variation in neutral plane position for transition through a stiffness discontinuity where ABD_1 is a laminate of [90,0] and ABD_2 is a laminate of [0,90]. The trend lines indicate the position of the neutral plane in the x direction as predicted by the UF-SLE model for various taper parameters $c = [0.1, 0.3, 0.5, 0.8, 1]$. The results predicted by CLT and the geometric mid-plane are provided for reference. A comparison with 3D-Ansys FEA is provided to illustrate accuracy of the UF-SLE model.

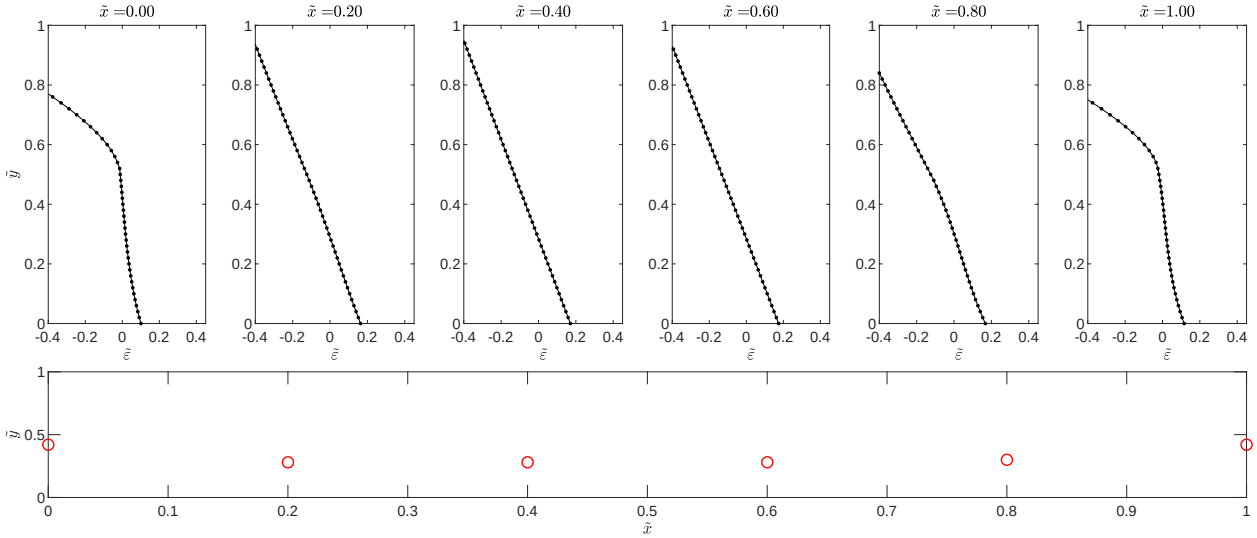

Fig. 8 Non-linear variation of normalised strain $\tilde{\varepsilon}$ predicted by UF-SLE, plotted through the thickness for normalised region $\tilde{x} \in [0, 1]$ with taper coefficient $c = 0.1$ including position of $\tilde{\varepsilon} = 0$.

the effect of geometric changes is smoothed over a region larger than the taper zone $\tilde{x} \in [0, 1]$.

Considering figure 9b, we observe the variation between the geometric mid-plane and the neutral plane position in the whole of the section. Both CLT and UF-SLE model predict this to the same extent in the constant thickness regions. However, in the tapered region, we observe some fundamental differences between the two approaches. We note that in the tapered region CLT does not predict a smooth variation in neutral plane position and it is instead affected by the relative stiffness of the plies. As with the zero ply laminate, the sharply tapered system smooths out the effects of both stiffness and geometry extending the effective range of the variation. In the extended taper cases, we observe a trend approaching the results predicted by CLT. For the cases between these two extreme cases the system responds in a mixed fashion, resulting in some unexpected features in the neutral plane position. There is an initial increase in height, but this is reversed as the geometric tapering begins. Features such as this are significant when predicting failure loads and we note that existing mechanisms to account for load path variations in CLT are unable capture such effects.

The final two cases, figures 9c and 9d, illustrate the importance of relative stiffness on the system. Although the two systems are symmetric in the constant thickness regions, significant levels of non-symmetry are introduced through the taper. We note that the laminate properties significantly affects the UF-SLE model predictions of neutral plane position. We observe that where the next additional ply is relatively stiff, i.e. 0°, the neutral axis position is increased. However, where the inclusion is a less stiff ply, i.e. 90°, the position of the neutral axis decreases. The nature of the transition is thus highly dependent on the stiffness of the system.

If we consider the geometric component of the eccentricity function, equation (6), as the length of taper is increased the rate of change of the eccentricity is reduced, smoothing out through-thickness effects over a longer region when accounting for the normalisation, as would be expected. Stiffness effects however appear to show localised features, in the form of the observed oscillations of the relative positions of the neutral plane. We observe that there is no oscillation observed in the $[0]_8$ laminate, figure 9a, having no stiffness variation through the thickness. Localisation, however is present in all the remaining cases figures 9b, 9c and 9d. Determining the length scale and magnitude of these oscillations of neutral axis position remains an open question. Interestingly, knowledge of this effect could be utilised to permit coupled stiffness/geometric tailoring of non-symmetric systems offering a route for elastic tailoring in the region that could significantly affect the level of through-thickness stresses in critical regions, e.g. stringer tip debonding.

C. Cubic

In the case of linear taper, we observed variations in the position of the neutral plane—predicted by the UF-SLE model—moving along the tapered region. For a linear taper the geometry is indeed continuous but its derivative is not. Equation (6), suggests that through-thickness effects can be compared to the rate of change of eccentricity. In order to avoid discontinuities in this geometric portion of this function, we propose a cubic taper profile that ensures C^1 smoothness of the transition. As shown in figure 10, we observe many of the features identified for the linear taper. This suggests that the repositioning of the neutral plane is indeed a physical effect and not a numerical artefact caused by geometric discontinuities. We note that the cubic taper geometry does affect behaviour. For example, by comparing figures 9d and 10d, we observe a smoother transition in the case of a cubic taper geometry. In particular, for the longer taper length, $c = 1$, the results match CLT predictions more closely than in the linear taper example.

V. Conclusions

In this paper, we present a comparison of neutral plane position, effective load path and through-thickness stress fields in tapered sections, representative of stringer terminations, ply drops, and tow steered plates. We compare the widely utilised CLT-based predictions with those of the Serendipity Lagrange Expansion (SLE)-based Unified Formulation (UF) model. In doing so, we observe how the rates of stiffness and geometric changes introduce localised variations not predicted by CLT, as would be expected due to its inherent two-dimensional assumptions. We also observe some unexpected reversal in changes to the relative height of the neutral plane for tapered geometries, and note the effect of relative stiffness on this effect.

It is common practice to account for geometric eccentricity in CLT smeared stiffness design approaches by using an effective eccentricity function to account for these geometric changes. Herein, we demonstrate that the effect of stiffness properties is significant in correctly predicting the true location of the neutral plane which defines the effective load path. This is significant due to the observation that for geometrically non-symmetric structures a non-symmetric stiffness distribution is typically created when tapering through the thickness, even where the initial and final laminates are themselves symmetric.

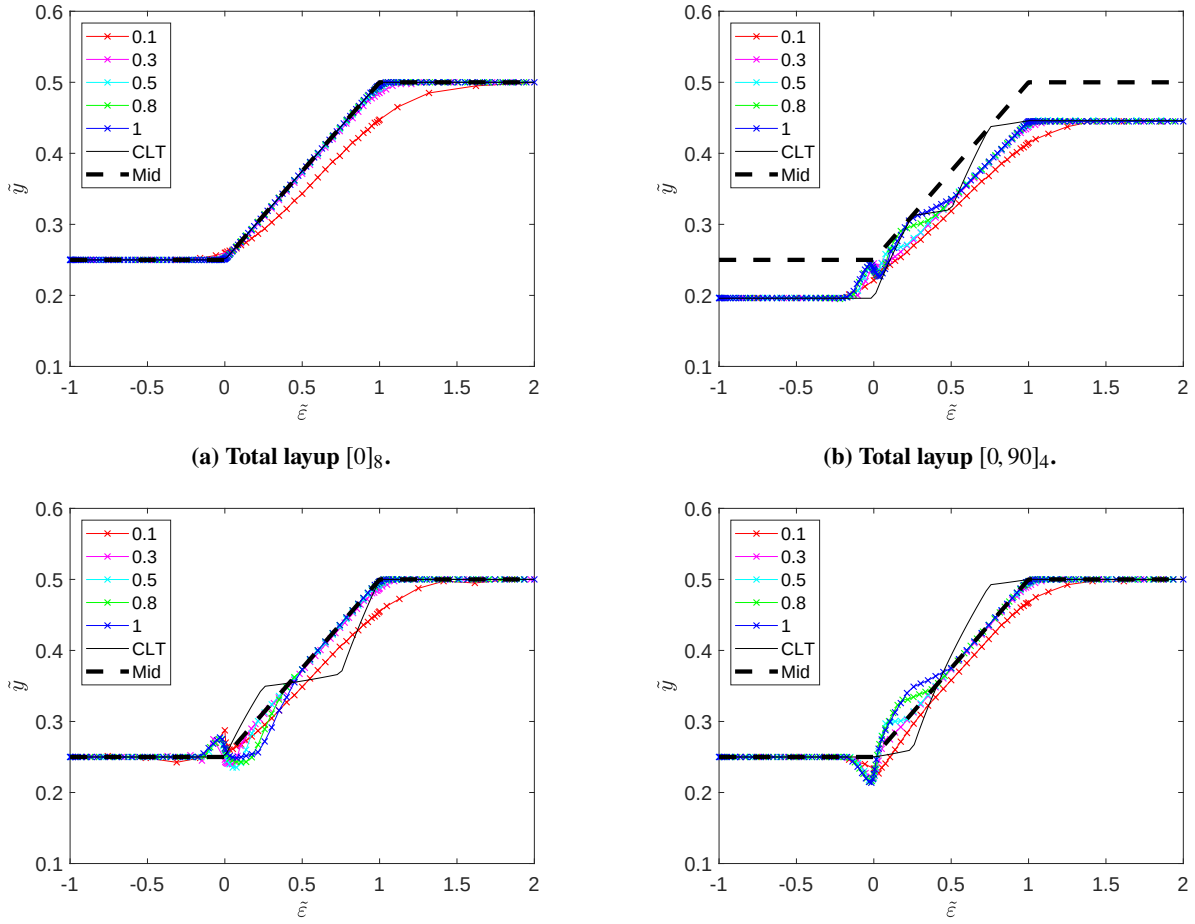

(a) Total layup $[0]_8$**.**

(b) Total layup $[0, 90]_4$**.**

(c) Total layup $[0, 90, 90, 0]_2$**.**

(d) Total layup $[90, 0, 0, 90]_2$**.**

Fig. 9 Linear taper geoemetry for various layups, the total layup i.e ABD$_C$ is indicated. The trend lines indicate the position of the neutral plane in the x direction as predicted by UF-SLE for various taper parameters $c = [0.1, 0.3, 0.5, 0.8, 1]$. The results predicted by CLT and the geometric mid-plane are provided for reference.

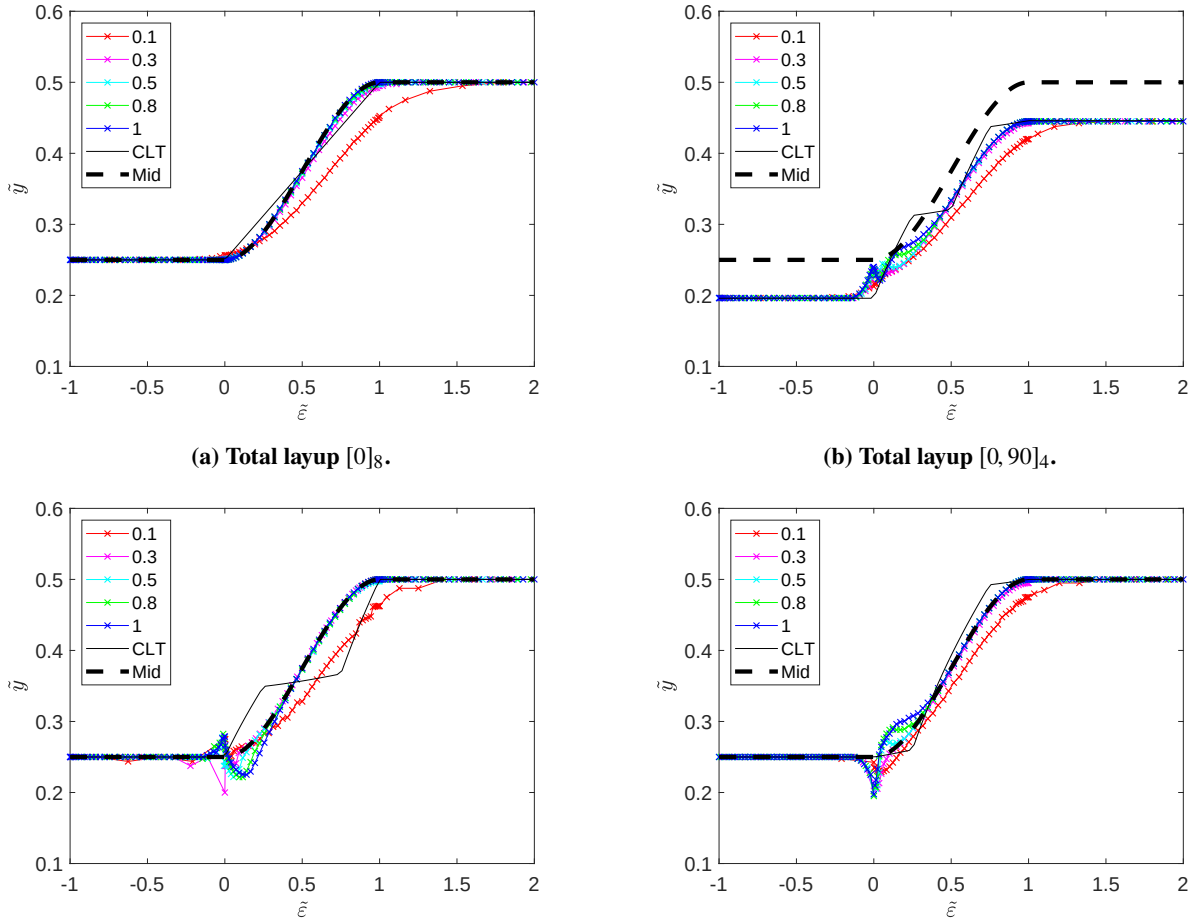

(a) Total layup $[0]_8$**.**

(b) Total layup $[0, 90]_4$**.**

(c) Total layup $[0, 90, 90, 0]_2$**.**

(d) Total layup $[90, 0, 0, 90]_2$**.**

Fig. 10 Cubic taper geometry for various layups. The trend lines indicate the position of the neutral plane in the x direction as predicted by UF-SLE for various taper parameters $c = [0.1, 0.3, 0.5, 0.8, 1]$. The results predicted by CLT and the geometric mid-plane is provided for reference.

Data Access Statement

The data necessary to support the conclusions are included in the paper.

Funding Sources

This research has been developed in the framework of the FULLCOMP project, supported by the H2020 Marie Skłodowska-Curie European Training Network [grant number 642121].

References

[1] Safety, A., "Status of FAA's actions to oversee the safety of composite airplanes," *US Government Accountability Office report: GAO-11–849*, 2011.

[2] Niu, C., *Airframe structural design: practical design information and data on aircraft structures*, Conmilit Press, 1988.

[3] Falzon, B., Davies, G., and Greenhalgh, E., "Failure of thick-skinned stiffener runout sections loaded in uniaxial compression," *Composite Structures*, Vol. 53, No. 2, 2001, pp. 223–233. doi:10.1016/S0263-8223(01)00006-X.

[4] O'Donnell, M., Weaver, P., and Cosentino, E., "Debond resisting composite stringers," *Collection of Technical Papers - AIAA/ASME/ASCE/AHS/ASC Structures, Structural Dynamics and Materials Conference*, 2012, p. 1.

[5] Hart-Smith, L., "Adhesive-Bonded Double-Lap Joints," Tech. rep., NASA, 1 1973.

[6] Cosentino, E., and Weaver, P. M., "Approximate nonlinear analysis method for debonding of skin stringer composite assemblies," *AIAA Journal*, Vol. 46, No. 5, 2008, pp. 1144–1159. doi:10.2514/1.31914.

[7] Cosentino, E., and Weaver, P. M., "Nonlinear Analytical Approach for Preliminary Sizing of Discrete Composite Stringer Terminations," *AIAA Journal*, Vol. 47, No. 3, 2009, pp. 606–617. doi:10.2514/1.37745.

[8] Carrera, E., "Theories and finite elements for multilayered, anisotropic, composite plates and shells," *Archives of Computational Methods in Engineering*, Vol. 9, No. 2, 2002, pp. 87–140. doi:10.1007/BF02736649.

[9] CARRERA, E., and GIUNTA, G., "Refined Beam Theories Based on a Unified Formulation," *International Journal of Applied Mechanics*, Vol. 02, No. 01, 2010, pp. 117–143. doi:10.1142/S1758825110000500.

[10] Minera, S., Patni, M., Carrera, E., Petrolo, M., Weaver, P. M., and Pirrera, A., "Three-dimensional stress analysis for beam-like structures using Serendipity Lagrange shape functions," *International Journal of Solids and Structures*, 2018. doi:10.1016/j.ijsolstr.2018.02.030.

[11] Patni, M., Minera, S., Groh, R. M. J., Weaver, P. M., and Pirrera, A., "Three-dimensional stress analysis for laminated composite and sandwich structures," *Composites Part B: Engineering*, Vol. 155, 2018, pp. 299–328. doi:10.1016/j.compositesb.2018.08.127.

[12] Patni, M., Minera, S., Weaver, P., and Pirrera, A., "A computationally efficient model for three-dimensional stress analysis of stiffened curved panels," *International Conference on Composite Materials and Structures, ICCMS 2017, Hyderabad, India*, 2017, p. 1.

[13] Mansfield, E. H., *The bending and stretching of plates*, 2nd ed., Cambridge University Press, Cambridge, UK, 2005.

[14] Gürdal, Z., Haftka, R. T., and Hajela, P., *Design and Optimization of Laminated Composite Materials*, Wiley-Interscience publication, Wiley, 1999.

[15] Nettles, A., "Basic Mechanics of Composite Plates," Tech. rep., NASA, 10 1994.

[16] Kumar, G., and Shapiro, V., "Efficient 3D analysis of laminate structures using ABD-equivalent material models," *Finite Elements in Analysis and Design*, Vol. 106, 2015, pp. 41 – 55. doi:https://doi.org/10.1016/j.finel.2015.07.009.

[17] Patni, M., Minera, S., Weaver, P., and Pirrera, A., "3D stress analysis for complex cross-section beams using unified formulation based on Serendipity Lagrange polynomial expansion," *3rd International Conference on Mechanics of Composites (MECHCOMP3), Bologna, Italy*, 2017, p. 1.